Cellular Microbiology (2008) **10**(1), 149–164
doi:10.1111/j.1462-5822.2007.01026.x
First published online 15 August 2007

Membrane cell fusion activity of the vaccinia virus A17–A27 protein complex

Grazyna Kochan,[1] David Escors,[2] José Manuel González,[1] Jose Maria Casasnovas[3] and Mariano Esteban[1]*
[1]*Department of Molecular and Cell Biology,*
[3]*Crystalization Unit of Department of Macromolecular Structures, Centro Nacional de Biotecnología, CSIC, Madrid, Spain.*
[2]*University College London, Windeyer Building, 46 Cleveland St, London W1T 4JF, UK.*

Summary

Vaccinia virus enters cells by endocytosis and via a membrane fusion mechanism mediated by viral envelope protein complexes. While several proteins have been implicated in the entry/fusion event, there is no direct proof for fusogenic activity of any viral protein in heterologous systems. Transient coexpression of A17 and A27 in mammalian cells led to syncytia formation in a pH-dependent manner, as ascertained by confocal fluorescent immunomicroscopy. The pH-dependent fusion activity was identified to reside in A17 amino-terminal ectodomain after overexpression in insect cells using recombinant baculoviruses. Through the use of A17 ectodomain deletion mutants, it was found that the domain important for fusion spanned between residues 18 and 34. To further characterize A17–A27 fusion activity in mammalian cells, 293T cell lines stably expressing A17, A27 or coexpressing both proteins were generated using lentivectors. A27 was exposed on the cell surface only when A17 was coexpressed. In addition, pH-dependent fusion activity was functionally demonstrated in mammalian cells by cytoplasmic transfer of fluorescent proteins, only when A17 and A27 were coexpressed. Bioinformatic tools were used to compare the putative A17–A27 protein complex with well-characterized fusion proteins. Finally, all experimental evidence was integrated into a working model for A17–A27-induced pH-dependent cell-to-cell fusion.

Received 9 May, 2007; revised 28 June, 2007; accepted 12 July, 2007. *For correspondence. E-mail mesteban@cnb.uam.es; Tel. (+34) 91 585 4553; Fax (+34) 91 585 4506.

Introduction

The *Poxviridae* family groups large and complex viruses that infect humans and animals causing severe diseases of clinical and veterinary importance, being the most representative variola virus the causative agent of smallpox. Vaccinia virus (VACV) is the best-characterized member of the family and contains a double-stranded DNA genome of 195 kb that encodes about 200 proteins (Moss, 2001). As a result of this complexity, many aspects of VACV infective cycle remain poorly characterized (Ericsson *et al*., 1995). In fact, VACV morphogenesis is very complex, and several forms are produced during virus infection: immature virus (IV), mature virions (MV), wrapped virions (WV) and envelope virions (EV) (Moss, 2006). The most abundant form is the MV, which acquires a membrane from the *trans*-Golgi compartment to form the WV, which is transported to the cell periphery, where the outermost membrane fuses and releases the EV (Smith and Vanderplasschen, 1998; Smith *et al*., 2002; Moss, 2006). MV and EV are the two infectious forms. VACV entry into host cells is mediated by two distinct pathways: at neutral pH by direct fusion with the cell membrane, and at acid pH by an endosomal route (Armstrong *et al*., 1973; Chang and Metz, 1976; Janeczko *et al*., 1987; Doms *et al*., 1990; Carter *et al*., 2005; Townsley *et al*., 2006). Biochemical, genetic and morphological data indicate that MV enter cells by a fusion mechanism, where the virus membrane fuses with the cell plasma membrane and releases the viral cores into the cytoplasm (Moss, 2006). In the case of EV, the outermost membrane is disrupted by a ligand-induced non-fusogenic reaction, and the inner viral membrane fuses with the plasma membrane (Law *et al*., 2006). At least 20 proteins are part of the MV membrane, while five proteins form the outer membrane of EV (Ericsson *et al*., 1995). Proteins A27, H3 and D8 initiate the virion attachment to the host cell by binding to glycosaminoglycans (Lai *et al*., 1990; Maa *et al*., 1990; Chung *et al*., 1998; Hsiao *et al*., 1999; Vazquez and Esteban, 1999; Lin *et al*., 2000). For fusion, several proteins have been implicated. Moss and coworkers used conditional lethal-null mutants to identify eight putative entry/fusion protein components (A21, L5, A28, H2, G3, G9, A16 and J5) as part of a large complex (Senkevich *et al*., 2004a,b; Senkevich *et al*., 2005; Townsley *et al*., 2005a,b; Ojeda *et al*., 2006). In these null

mutants the MV can bind to cells, although it fails to trigger fusion and penetration (Moss, 2006). On the other hand, earlier studies by our group implicated the trimeric membrane protein A27 with a role in fusion using neutralizing and fusion-blocking antibodies (Rodriguez and Esteban, 1987; Rodriguez *et al*., 1987; Gong *et al*., 1990; Vazquez and Esteban, 1999). In addition, A27 was found in VACV-infected cells to form a complex with two other membrane proteins, A14 and A17, both of which are critical players in the formation of viral membranes (Rodriguez and Esteban, 1987; Rodriguez *et al*., 1987; 1993; 1995; 1997; 1998; Gong *et al*., 1990; Rodriguez and Smith, 1990; Wolffe *et al*., 1996; Vazquez and Esteban, 1999). While it was shown that A27 and A17 directly interacted through the C-terminal α-helix (Vazquez *et al*., 1998), there was also interaction between A17 and A14 (Rodriguez *et al*., 1997; Mercer and Traktman, 2003). In particular, A17 is an integral membrane protein that associates with the endoplasmic reticulum membranes, and VACV mutants lacking A17 or A14 do not produce MV and accumulate membrane vesicles and tubules in the cytoplasm (Rodriguez and Smith, 1990; Krijnse-Locker *et al*., 1996; Wolffe *et al*., 1996; Rodriguez *et al*., 1997; 1998; Betakova *et al*., 1999; Betakova and Moss, 2000; Wallengren *et al*., 2001). In contrast, VACV mutants lacking A27 formed normal MV but not WV (Rodriguez and Smith, 1990), and A27-null mutants in the form of MV were able to induce membrane fusion. Therefore, it was suggested that A27 was not a fusion protein (Senkevich and Moss, 2005).

Previous studies have indicated the complexity of poxvirus entry/fusion. As yet, a poxvirus protein(s) directly responsible for triggering cell fusion in the absence of viral infection has not been identified. Using transfection assays, a baculovirus expression system and a lentivirus-based expression system, we found that VACV protein complex A17–A27 induced pH-dependent cell fusion. Fusion activity was demonstrated by confocal immunomicroscopy and a functional quantitative assay based on cytoplasmic transfer of fluorescent proteins. The fusion activity resided in A17 ectodomain between residues 18 and 34. A working model compatible with the experimental data is proposed, and the classification of A17–A27 as a fusion complex is discussed.

Results

Coexpression of A17 and A27 in human 293T cells results in pH-induced cell fusion

We previously reported that VACV-induced cell fusion was blocked by A27-specific mAbs and virus–cell binding by peptides to amino acids 21–33 of A27 (Rodriguez *et al*., 1987; Vazquez and Esteban, 1999). On the other hand, it was recently shown that a VACV mutant lacking A27 gene triggered pH-induced fusion from without (Senkevich and Moss, 2005). Thus, we hypothesized that an additional protein could participate in fusion activity together with A27. To test this hypothesis, human 293T cells were transfected with expression plasmids encoding A27 and A17 (the natural partner of A17 in VACV membrane). Low pH-triggered fusion was induced, and fusion activity was analysed by confocal immunofluorescence microscopy using A17- and A27-specific antibodies (Fig. 1A and B). While expression of A17 or A27 failed to induce fusion, coexpression of both led to syncytia containing several nuclei only after acid pH treatment (Fig. 1). Furthermore, over 70% of cells synthesizing both proteins were forming syncytia (Fig. 1C). However, the low coexpression efficiencies achieved by transient transfection precluded further studies (Fig. 1C).

A17 expression in insect cells by recombinant baculoviruses results in pH-dependent cell-to-cell fusion comparable to A17 and A27 coexpression

Powerful heterologous recombinant virus vectors such as baculovirus (Kochan *et al*., 1993; 2003) have been previously used to characterize fusion proteins (Gething *et al*., 1986; Forzan *et al*., 2004). Therefore, A17 and A27 genes were expressed in insect cells using recombinant baculoviruses. The A17 signal peptide was replaced by baculovirus gp64 signal peptide to generate an A17 N-terminus identical to that found after proteolytic processing in VACV-infected cells. A17 and A27 proteins were accumulated at high levels in insect cells after infection with the indicated baculoviruses as determined by immunoblot with specific antibodies (Fig. 2A). Interestingly, baculovirus-expressed A27 presented two sizes, 14 and 12 kDa, suggesting that this protein was processed in insect cells similarly to bacterial expression systems and in VACV-infected cells, as previously reported (Fig. 2A) (Lai *et al*., 1990; Vazquez *et al*., 1998). Unprocessed A17 has a predicted size of 23 kDa that is rapidly processed to 21 kDa in VACV-infected cells, with the N- and C-termini modified by proteolytic cleavages (Rodriguez *et al*., 1993; Rodriguez *et al*., 1996; Betakova *et al*., 1999; Betakova and Moss, 2000; Wallengren *et al*., 2001). Baculovirus-expressed A17 showed the same size as found in VACV-infected cells (Fig. 2A).

Extensive fusion activity was observed after acid pH shift when A17 and A27 were coexpressed, but not when cells were infected with baculovirus encoding only A27 (Fig. 2B) or in control baculovirus-infected cells (not shown), as determined by confocal fluorescence immunomicroscopy (Fig. 2B). Surprisingly, A17 expression was sufficient to induce pH-dependent cell fusion at

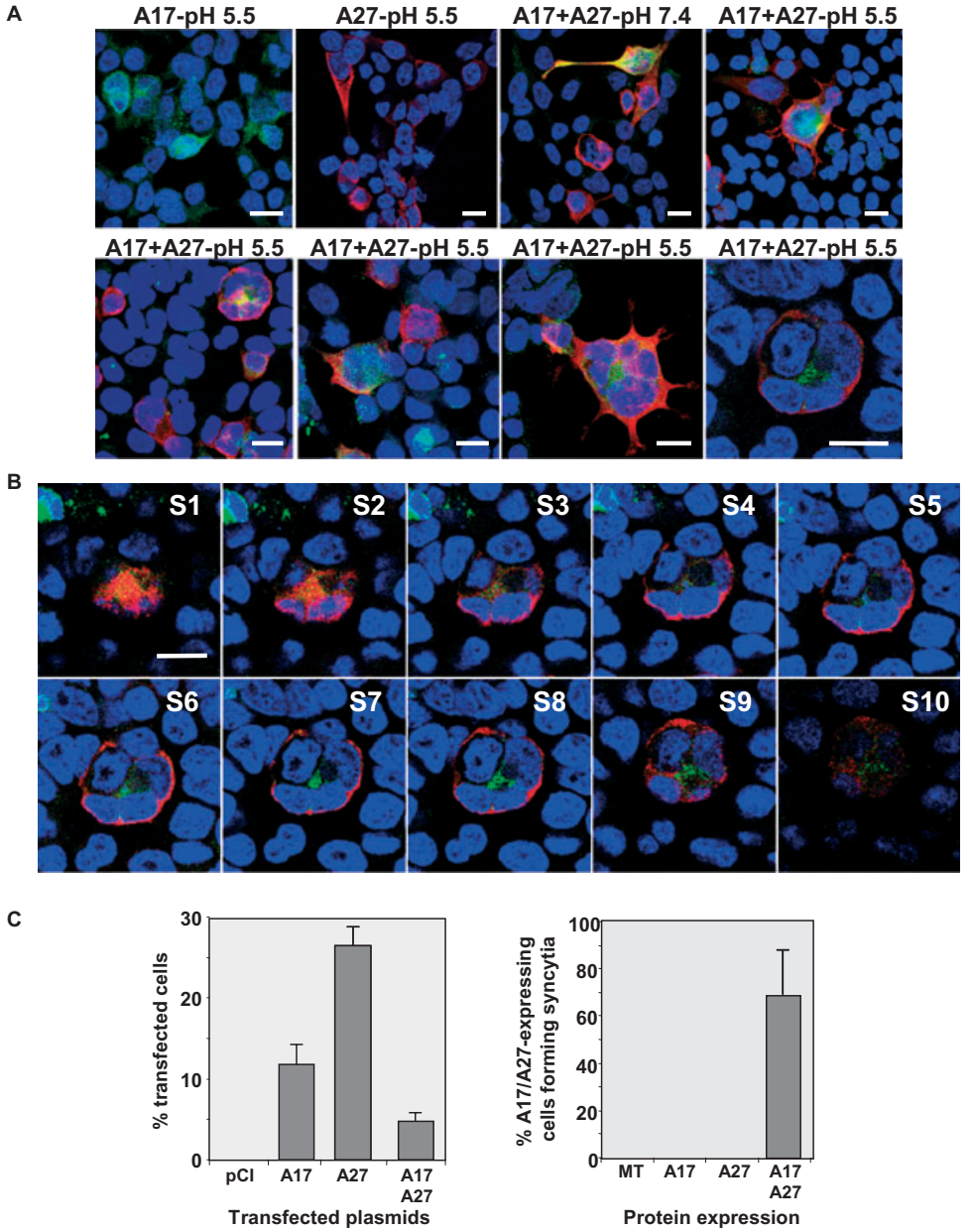

Fig. 1. Cell-to-cell fusion at acid pH mediated by the A17 and A27 complex in human cells. Human 293T cells were transfected with pCIneo plasmids encoding A17 and A27 genes, separately or in combination. At 72 h post transfection, cells were exposed to low pH (pH 5.5) or neutral (pH 7.4) for 3 min. After further incubation in medium for 6 h, cells were fixed, permeabilized and processed for confocal fluorescence immunomicroscopy, using A17- and A27-specific antibodies, followed by rhodamine-conjugated rabbit anti-mouse (A27, red) or fluorescein isotiocyanate-conjugated goat anti-rabbit antibodies (A17, green). DNA was visualized by ToPro staining. Presented images are sections of monolayer cell cultures.

A. Panels show confocal fluorescent immunomicroscopy pictures of cells transfected with pCIneo plasmids encoding the indicated proteins on top, at different magnifications. The pH to which cells were exposed is also indicated. Only cells expressing both A17 and A27 genes formed syncytia after a low-pH treatment. The lower panels show different representative syncytia coexpressing A17 and A27 at varying magnifications containing more than four nuclei. Bars within each panel represent 25 μm. A17 is labelled in green, while A27 is labelled in red. Colocalization of both proteins is shown in yellow.

B. Sections (S) of a single representative syncytium coexpressing A17 and A27 from a panel in (A), where the continuity of cell membranes in syncytium is observed. Bar within the upper left panel represents 25 μm.

C. Left graph represents transfection efficiencies with pCIneo expressing A27, A17 and A17 + A27 respectively, as determined by immunofluorescence microscopy. Efficiencies were calculated from 700 randomly chosen cells in each transfection. Right graph shows the percentage of A17/A27-expressing cells forming syncytia after pH treatment in transfected cells as indicated below the graph. Close to 70% of cells coexpressing A17 and A27 were forming syncytia. No syncytium formation was observed when A17 or A27 was exclusively expressed. pCI, pCIneo plasmid; MT, mock transfected cells.

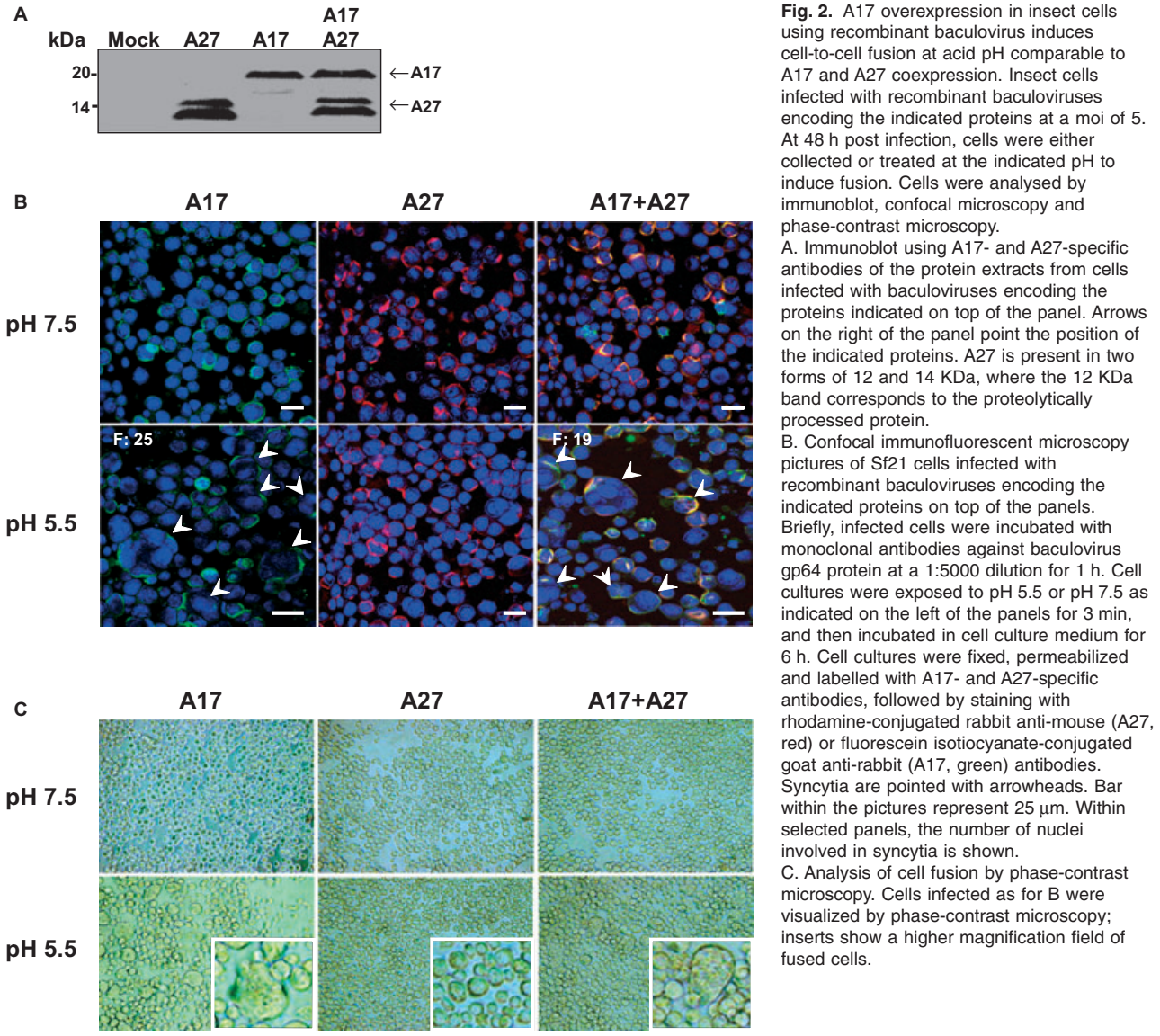

Fig. 2. A17 overexpression in insect cells using recombinant baculovirus induces cell-to-cell fusion at acid pH comparable to A17 and A27 coexpression. Insect cells infected with recombinant baculoviruses encoding the indicated proteins at a moi of 5. At 48 h post infection, cells were either collected or treated at the indicated pH to induce fusion. Cells were analysed by immunoblot, confocal microscopy and phase-contrast microscopy.
A. Immunoblot using A17- and A27-specific antibodies of the protein extracts from cells infected with baculoviruses encoding the proteins indicated on top of the panel. Arrows on the right of the panel point the position of the indicated proteins. A27 is present in two forms of 12 and 14 KDa, where the 12 KDa band corresponds to the proteolytically processed protein.
B. Confocal immunofluorescent microscopy pictures of Sf21 cells infected with recombinant baculoviruses encoding the indicated proteins on top of the panels. Briefly, infected cells were incubated with monoclonal antibodies against baculovirus gp64 protein at a 1:5000 dilution for 1 h. Cell cultures were exposed to pH 5.5 or pH 7.5 as indicated on the left of the panels for 3 min, and then incubated in cell culture medium for 6 h. Cell cultures were fixed, permeabilized and labelled with A17- and A27-specific antibodies, followed by staining with rhodamine-conjugated rabbit anti-mouse (A27, red) or fluorescein isotiocyanate-conjugated goat anti-rabbit (A17, green) antibodies. Syncytia are pointed with arrowheads. Bar within the pictures represent 25 μm. Within selected panels, the number of nuclei involved in syncytia is shown.
C. Analysis of cell fusion by phase-contrast microscopy. Cells infected as for B were visualized by phase-contrast microscopy; inserts show a higher magnification field of fused cells.

comparable levels to those triggered by A17–A27 coexpression (Fig. 2B). These results suggested that A17 overexpression in insect cells was sufficient to induce pH-dependent cell fusion. Therefore, we concluded that the domain responsible for fusion activity resided in A17.

Fusion activity of A17 is localized in the N-terminal ectodomain

To identify the A17 region responsible for fusion activity, a collection of deletion mutants covering the N-terminal ectodomain were generated and expressed in insect cells (Fig. 3A). A17 mutants were expressed at comparable levels as shown by immunoblot (Fig. 3B). First, it was confirmed that A17 mutant proteins were exposed on the cell surface in non-permeabilized infected cells by surface staining with A17-specific antibodies and flow cytometry (Fig. 3C). A significant increase in the number of A17-labelled cells was observed compared with control baculovirus-infected cells that produced levels comparable to isotype controls (Fig. 3C). Second, the fusion activity of each mutant was assayed by confocal immunofluorescence microscopy and quantification of the number of syncytia per total nuclei (Fig. 4). Cells expressing A27 were used as a negative control, because they did not induce cell-to-cell fusion (Fig. 2B). Mutants with deletions covering residues from 31 to 59 showed fusion activity statistically comparable to wild-type A17 ($P = 0.55$). In contrast, removal of residues 18–25 or 21–34, or a point mutation in residue 23 (D→N), significantly abrogated fusion activity (around an 80% decrease) ($P = 0.008$) (Fig. 4B). These results strongly suggested that region

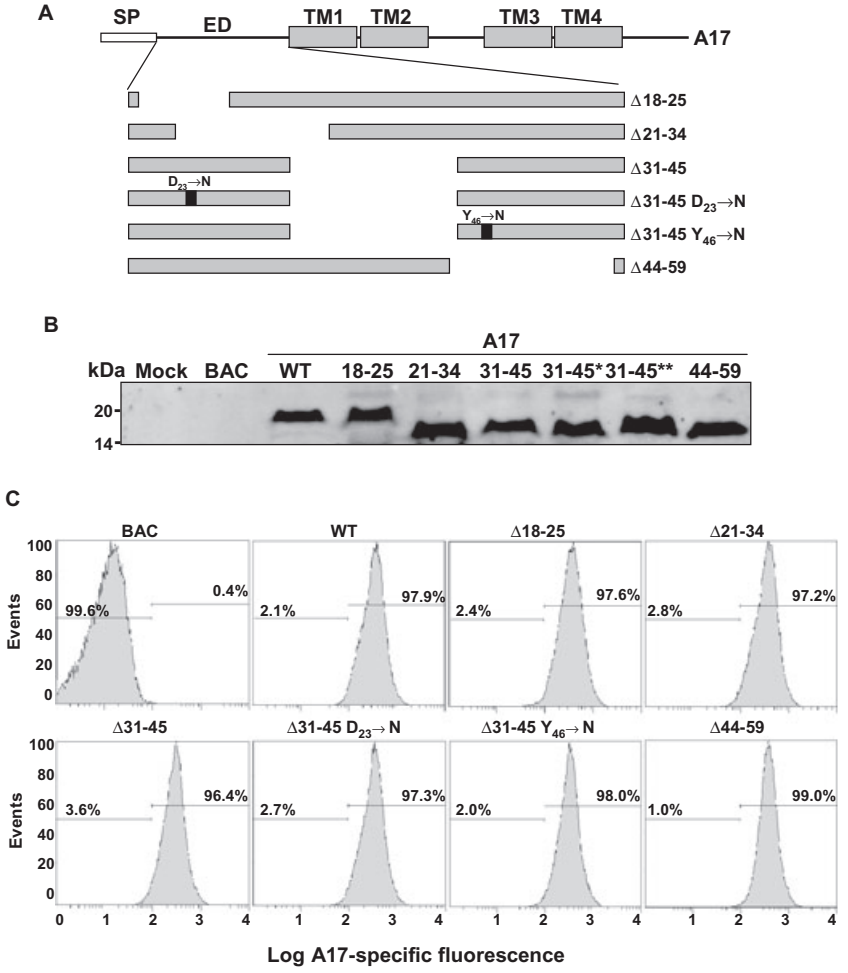

Fig. 3. Expression of A17 deletion mutants.
A. A scheme of A17 gene is shown as a bar, with regions encoding the signal peptide (SP), ectodomain (ED) and predicted transmembrane domains (TM), as indicated on top of the bar. Schemes indicating the structure of the ectodomain deletions are shown below the A17 gene. Mutant names are indicated on the right of each bar, with the numbers indicating the last and the first amino acids flanking deletions. Single amino acid substitutions in mutants Δ31-45 D_{23}→N and Δ31-45 Y_{46}→N are indicated by black boxes within the bars, and the amino-acid change is shown above.
B. Expression of A17 mutants in Sf21 cells infected with recombinant baculoviruses was assessed by immunoblot using A17-specific antibodies. All mutants were efficiently expressed and showed the expected size.
C. Non-permeabilized insect cells infected with recombinant baculoviruses encoding the indicated A17 deletion mutants (top of the graphs) were labelled by surface staining using A17-specific antibodies, and FITC-conjugated antibodies, as described in *Experimental procedures*. Stained viable cells were analysed by flow cytometry. Horizontal lines represent gates established by exclusion of 99% (left bar) of stained negative control wild-type baculovirus-infected cells, and inclusion of less than 1% (right bar). Percentages of cells within each gate are shown above the bars. Graphs were represented as histograms showing the number of cells as a function of specific A17 fluorescence in a logarithmic scale. BAC represents control baculovirus; WT represents recombinant baculovirus encoding wild-type A17; Wild-type A17 and its deletion mutants were exposed on the cell surface of infected insect cells.

responsible for fusion activity was located between residues 18 and 34 in the A17 ectodomain.

Intracellularly retained A27 is transported to the cell surface when A17 is coexpressed in human cells

The data obtained from transient transfections in mammalian cells and in insect cells using recombinant baculoviruses suggested that A17 and A27 induced cell-to-cell fusion. However, low co-transfection efficiencies prevented further characterization of fusion in mammalian cells. Thus, HIV-1-based lentivectors encoding each gene were used to generate 293T cells stably expressing these genes, because lentivectors integrate into the cell genome, leading to a sustained and long-term transgene expression (Collins and Cerundolo, 2004). Therefore, A17 and A27 genes were cloned under the control of the spleen focus-forming virus (SFFV) promoter in a self-inactivating lentivector previously described (Fig. 5A), and lentivector preparations were obtained and titrated as described (Rowe *et al.*, 2006; Selden *et al.*, 2007). Expression of A17 and A27 after transduction with lentivectors was confirmed by immunoblot using specific antibodies (Fig. 5A). Cultures were routinely kept for around 1 month to perform experiments. The percentage of cells expressing both proteins after co-transduction with lentivectors was assessed by intracellular double staining with A17- and A27-specific antibodies. As controls, cell lines stably expressing only A17 or A27 were generated. Around 30% of cells expressed A17 when transduced with a lentivector encoding A17 (Fig. 5B). Consequently, around 60% of cells transduced with the lentivector encoding A27 expressed A27 (Fig. 5B). Finally, 20% of cells co-transduced with lentivectors encoding A17 and A27 coexpressed both proteins, while around 30% expressed A17 only and 5% only A27 (Fig. 5B).

Previous data suggested that A17 and A27 are present on the cell surface as a complex. To confirm this, surface staining of non-permeabilized transduced 293T cells coexpressing A17 and A27 was performed using specific antibodies, and analysed by flow cytometry. A17 was specifically detected on the surface of cells expressing A17 or coexpressing A17 with A27, as determined by the number of labelled cells and mean fluorescent intensities

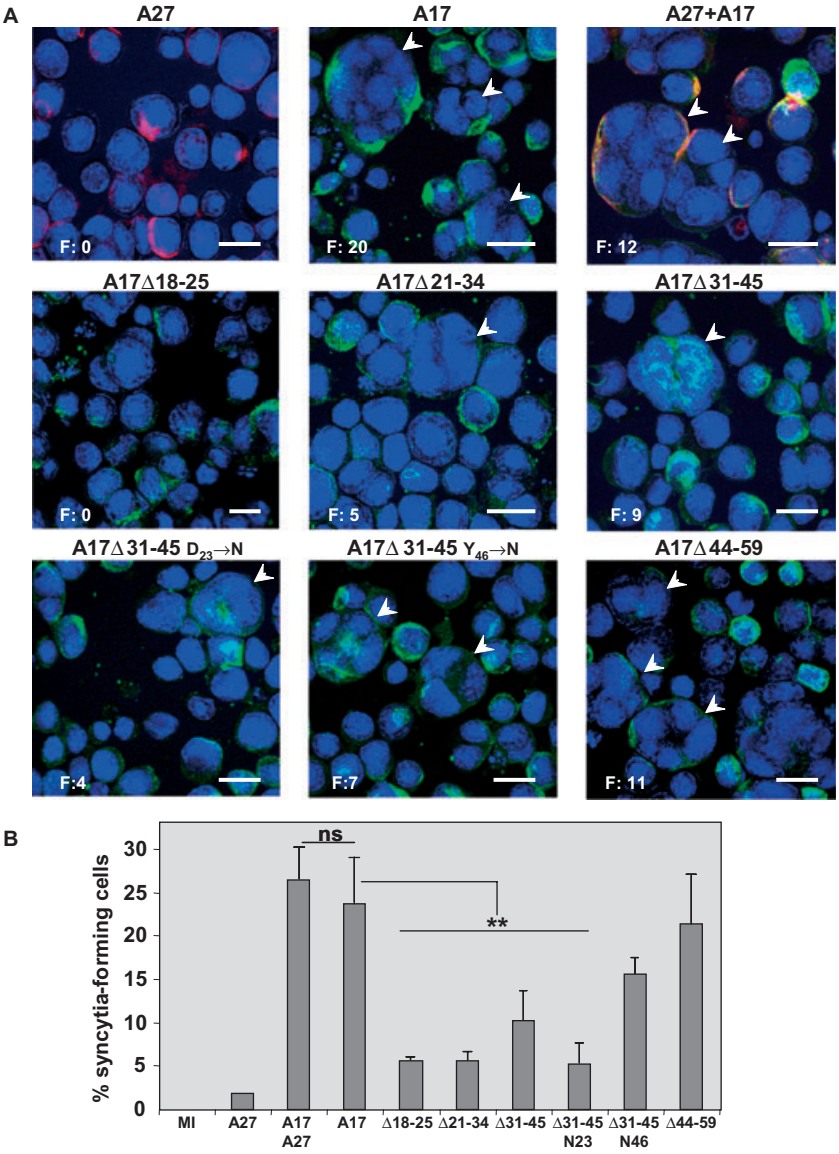

Fig. 4. Fusion activity resides in A17 ectodomain.
A. Fusion assays were carried out in insect cells infected with recombinant baculoviruses encoding the indicated A17 mutants, following the same conditions as in Fig. 2. Panels show some examples of confocal immunomicroscopy pictures from the fusion assays. Syncytia within each panel are pointed with arrowheads. The number of nuclei involved in syncytia formation is shown within each panel. Bars within each panel represent 25 μm.
B. The graph represents means from percentages of fused cells (nuclei involved in syncytia per 100 total nuclei), calculated for each A17 mutant. Means are represented as column bars with error bars (standard deviations). In each case, data were obtained from 3000 randomly counted total nuclei. Selected statistical comparisons are shown within the graph, and the *P*-values were calculated using the parametric ANOVA test for multiple comparisons, and the Tukey two-paired comparison test when appropriate. ns, no significant differences ($P > 0.5$); **significant differences ($P < 0.1$). MI, mock infection.

(Fig. 5C). In contrast, A27 was specifically detected on the cell surface only when both A17 and A27 were coexpressed. These data are in agreement with an intracellular specific interaction between these two proteins and transport to the cell surface.

Functional characterization of cell-to-cell fusion by cytoplasmic transfer of fluorescent proteins mediated by A17 and A27

Fusion activity in mammalian (transient transfection) and insect cells (recombinant baculovirus) by A17 and A27 was exclusively based on microscopic observations. Although unlikely, it cannot be discarded that syncytia of A27- and A17-expressing 293T cells could be the result of a faulty cell division rather than a pH-induced fusion. To discard this possibility and quantitatively prove that A17 and A27 mediated pH-dependent cell-to-cell fusion, a GFP–RFP cytoplasmic transfer assay was developed (Fig. 6A). For this purpose, independent 293T cell lines stably expressing GFP or RFP were co-transduced with lentivectors encoding A17 and A27, and kept in culture. Then, cells were detached by pipetting from the plates and mixed. Two hours after mixing, pH-induced fusion was performed, and living cells were analysed 2 h later by confocal fluorescence microscopy. No detectable effects were observed when 293T cells expressing only GFP or RFP were mixed and subjected to acid pH (Fig. 6B). In contrast, significant cell aggregation was observed when cells were coexpressing A17 and A27 and subjected to acid pH. Closer examination showed that approximately 30–40% of cells were forming syncytia, from which

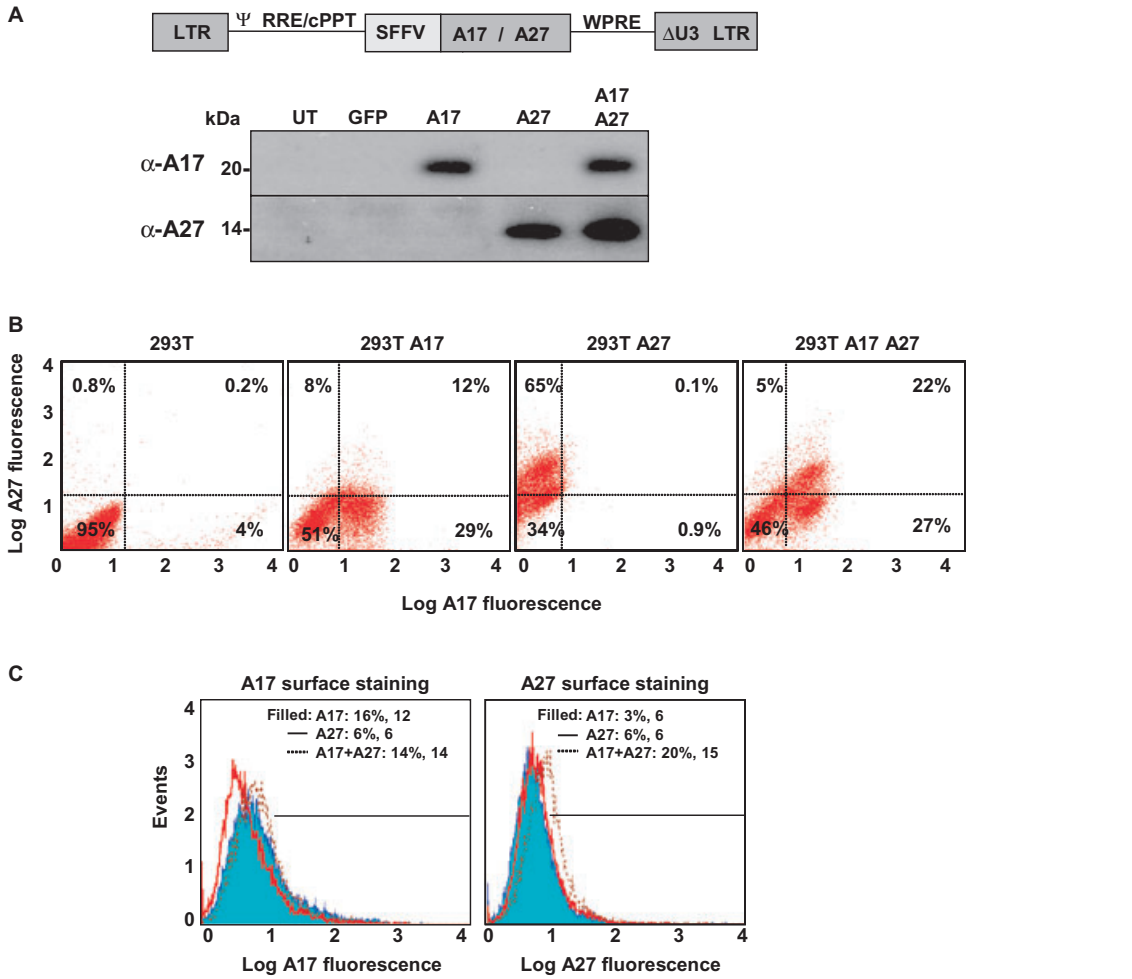

Fig. 5. Stable expression of A17 and A27 in 293T cells using lentivectors.
A. Lentivectors encoding A17 or A27 were generated. The lentivector structure is shown: LTR, HIV-1 long-terminal repeat; ψ, HIV packaging signal; RRE, HIV Rev response element; cPPT, HIV central polypurine tract; WPRE, woodchuck hepatitis virus post-transcriptional regulatory element; UBIQ, human ubiquitin promoter. ΔU3 represents the HIV-1 LTR with a deletion covering the U3 region, resulting in a SIN lentivector. Below, A17 and A27 expression was confirmed in 293T cells transduced with the indicated lentivectors by immunoblot using A17- and A27-specific antibodies. Briefly, 293T cells were transduced with the indicated lentivectors at a moi of 20. 293T cells were kept in cell culture, and stable A17 and A27 expression was confirmed up to 1 month.
B. Permeabilized 293T cells stably expressing A17, A27 or A17 + A27 were stained with A17- and A27-specific antibodies. Data are represented as dot plots from flow cytometry analyses for A17 and A27 in 293T cells expressing the indicated proteins (top of each panel). PE (for A27) fluorescence levels (*y*-axis) were represented as a function of FITC (for A17) fluorescence (*x*-axis). Quadrants were established based on background fluorescence of each antibody in untransduced 293T cells. Percentage of cells within each quadrant is indicated. Around 20% of cells co-transduced with lentivectors encoding A17 and A27 actually coexpressed both proteins.
C. Non-permeabilized 293T cells stably expressing A17, A27 or A17 + A27 were labeled with A17- or A27-specific antibodies by surface staining. Data are shown as histograms representing the number of cells as a function of A17- or A27-specific fluorescent in a logarithmic scale. Horizontal lines represent gates established by exclusion of 95% of stained untransduced 293T cells, and inclusion of less than 5% (within the line). Percentages of cells within the gate and mean fluorescent intensities are shown above the bars. The results showed that in non-permeabilized cells, A27 is found on the cell surface only when it is coexpressed with A17. This is found in a 20% of cells co-transduced with lentivectors encoding A17 and A27, in agreement with the data obtained by intracellular staining (B). This suggests that A27 binds to A17 intracellularly and both proteins are exposed as a complex.

around a third contained both GFP and RFP (Fig. 6C). The number of syncytia was in agreement with the proportion of cells coexpressing A17 and A27 (Fig. 5B and C). In addition, this result strongly suggested that cytoplasmic transfer was taking place most likely through direct cell-to-cell fusion. The number of GFP^+ RFP^+ syncytia was quantified by flow cytometry, detecting RFP fluorescence in GFP-containing cells (Fig. 7). As expected, no significant detection of GFP^+ RFP^+ cells (events) was detected when cells were only expressing GFP and RFP after a pH drop (Fig. 7A). No specific detection of GFP^+ RFP^+ cells was observed when A17 or A27 was singly expressed after a pH drop (Fig. 7B and C). In contrast, a well-defined population of GFP^+ RFP^+ cells

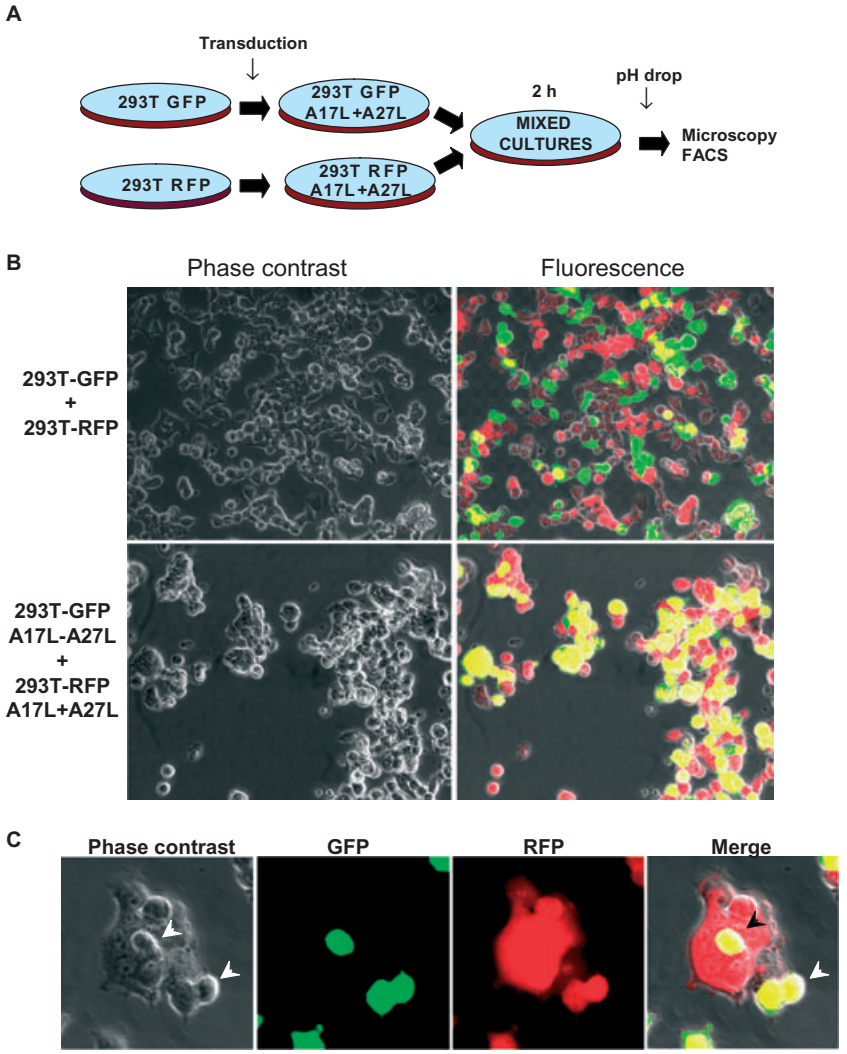

Fig. 6. A17–A27-mediated cytoplasmic cell transfer of GFP- and RFP-expressing cells.
A. A functional quantitative fusion assay based on cytoplasmic transfer of fluorescent proteins was set up and schematically shown in the figure. Briefly, 293T cells expressing either GFP or RFP were transduced with lentivectors encoding A17 and A27, and kept in culture for variable amounts of time. Then, both independent lines were mixed and allowed to attach to a new culture plate for at least 2 h. Fusion was then induced by a pH drop, and cell fusion analyses were performed around 2 h later.
B. A17–A27-expressing 293T cells containing either GFP or RFP were mixed, and fusion was induced as explained above. Living cells were analysed by confocal fluorescent microscopy, and representative pictures are shown. Phase-contrast pictures exclusively or including GFP and RFP detection are shown as indicated on top of the panels. GFP- and RFP-containing cells without A17 and A27 expression were carried out as negative controls. GFP is shown in green, RFP in red, and GFP + RFP (merge) is shown in yellow. A17 and A27 coexpression induces cell aggregation and fusion 2 h after the pH drop, but not control cells.
C. One representative syncytium is shown while it is forming, either at phase-contrast, GFP detection, RFP detection and merge. Arrowheads indicate GFP-containing cells fusing with RFP-containing cells.

(around 10%) was detected in cells coexpressing A17 and A27 only when a pH drop was performed (Fig. 7D). This number was in close agreement with one-third of the expected syncytia to be GFP^+ RFP^+. Therefore, the results from stable expression using lentivectors suggested that A17 and A27 were present as a complex on the cell surface when coexpressed. By cytoplasmic transfer of fluorescent proteins, it was shown that both proteins were required to induce pH-triggered cell-to-cell fusion in mammalian cells.

Predicted primary and secondary structures of A17 and A27 suggest a mechanism for A17-induced fusion

Sequence conservation is usually an indicator of functional importance, and Wimley–White interfacial hydrophobicity scores, which measure a peptide's ability for membrane partitioning, and the Kyte–Doolittle hydropathy scale have been previously used to identify viral fusion peptides (Kyte and Doolittle, 1982; Wimley and White, 1996; Wimley *et al.*, 1996; Nieva and Suarez, 2000).

A multiple sequence alignment (Fig. 8A) showed that A17 is specially conserved in the identified fusion domain (residues 18–34) and the A27 binding domain. In addition, the fusion domain high-sequence conservation and the presence of two completely conserved phenylalanine residues, which are bulky residues typically found in fusion peptides, support its role as a fusion peptide. Interestingly, hydrophobicity plots of A17 ectodomain at neutral pH using MPEx (Jaysinghe, 2006) (Fig. 8B) indicate a small tendency for the fusion domain to get into the membrane–polar interface. Most interestingly, its tendency is increased at low pH where glutamic and aspartic residues are neutral, which would suggest a mechanistic explanation for pH-induced cell-to-cell fusion. Similar cases for viral fusion proteins have been documented (Nieva and Suarez, 2000). This is the case of reovirus fusion-associated small transmembrane protein (FAST)

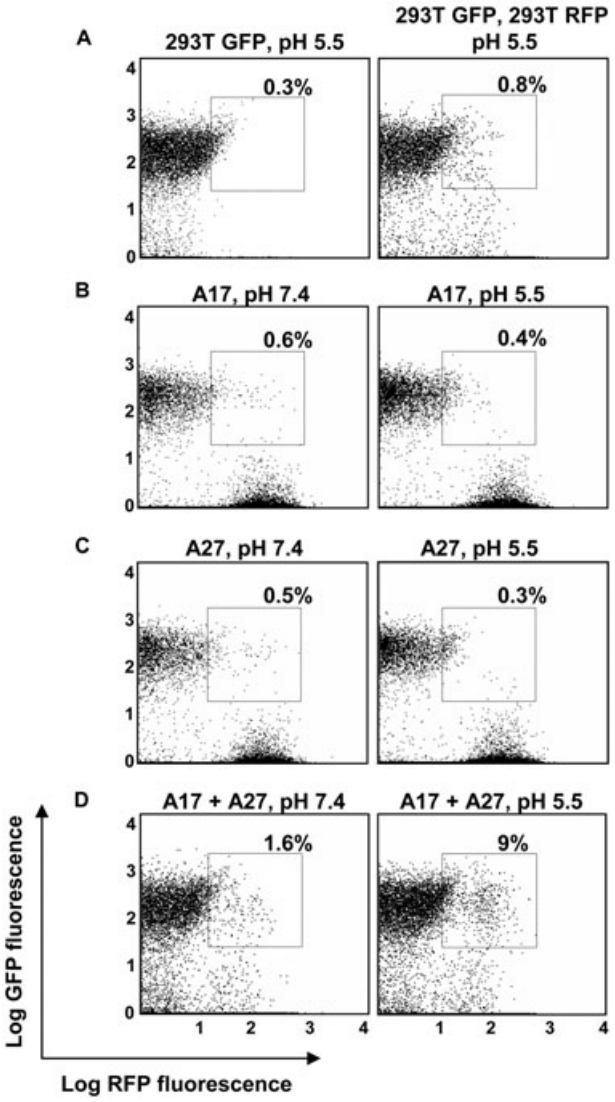

Fig. 7. Quantification of GFP$^+$ RFP$^+$ 293T cells after A17–A27-mediated cell fusion and cytoplasmic transfer. 293T cells expressing either GFP or RFP were transduced with lentivectors encoding A17 and A27, and kept in culture for variable amounts of time. Then, cells were mixed as described in Fig. 6 and fusion was induced by a pH drop. RFP transfer into GFP-containing cells was quantified by flow cytometry. Panels show dot plots from GFP-containing cells, representing GFP fluorescence as a function of RFP fluorescence in logarithmic scale.
A. Dot plots from cells containing GFP only (left panel) or GFP and RFP (right panel) after a pH drop.
B. Dot plots from mixed cells containing GFP or RFP and expressing A17 only. The left panel shows treatment with neutral pH, and the right panel after a pH drop.
C. As in (B), but with cells expressing A27 only, or (D) coexpressing A17 and A27. These are representative results from three independent experiments. The results show that, only when A17 and A27 are coexpressed, there is evident and significant RFP transfer into GFP-containing cells. This represents a well-defined cell (syncytia) population, accounting for a 10% of total cells (events). This would represent approximately one-third of the expected total syncytia that would include only GFP or RFP.

that shows moderate hydrophobicity scores, compensated by a myristate moiety and a protruding loop (Corcoran *et al*., 2004) (Fig. 8B). In the case of A17, it cannot be discarded that the fusion domain can adopt a structure that allows its insertion into the membrane interface.

Secondary structure prediction for A17 showed that N- and C-termini are mostly random coiled, while there was a central hydrophobic region (residues 60–157) which could contain two or four transmembrane domains (Figs 3A and 8A) (Krijnse-Locker *et al*., 1996; Betakova *et al*., 1999; Betakova and Moss, 2000). A17 ectodomain spans residues 17–59 after signal peptide removal in VACV-infected cells, and it is present on the cytoplasmic site of IV membranes (Krijnse-Locker *et al*., 1996; Wolffe *et al*., 1996). It contains two short regions predicted to be helical. One corresponds to a conserved stretch of polar/charged amino acids within the identified domain important for fusion (residues 27–32). The other is located close to the first transmembrane domain (residues 48–57), where the A27 binding domain has been mapped (Vazquez *et al*., 1998). Further attempts to predict the tertiary structure of A17 ectodomain through fold recognition using Genesilico (Kurowski and Bujnicki, 2003) or *ab initio* by Robetta (Kim *et al*., 2004) proved to be unreliable.

A27, which contributed to fusion activity, is a conserved protein in poxviruses (Fig. 8C). The A27 N-terminus presents a random-coiled structure, including the glycosaminglycan binding domain (residues 21–32), while the rest of the protein is mainly helical, as previously shown by nuclear magnetic resonance and circular dichroism (Vazquez *et al*., 1998; Lin *et al*., 2002). The central domain (residues 44–72) is an α-helix with high tendency to form coiled-coil trimers (Vazquez *et al*., 1998; Lin *et al*., 2002), and the C-terminus contains a predicted leucine zipper motif (positions 77–98). The A27 carboxy terminus is highly conserved in poxviruses, and is essential for A17 binding. Therefore, A27 exposure only when coexpressed with A17 is most likely due to an intracellular A17–A27 binding and transport to the cell surface (Fig. 5B and C). According to the data from mammalian cells, only when both proteins are present on the surface, pH-dependent cell-to-cell fusion is observed, both by microscopy and by functional fusion assays based on cytoplasmic transfer of fluorescent proteins. Therefore, A17 and A27 would be forming a complex in which A27 contains a glycosaminoglycan binding domain, while A17 would remain physically anchored in the cell membrane containing the fusion peptide.

Discussion

Despite the high heterogeneity of fusion proteins of different virus groups, the viral membrane-fusion process involves only a single fusion component as shown in the

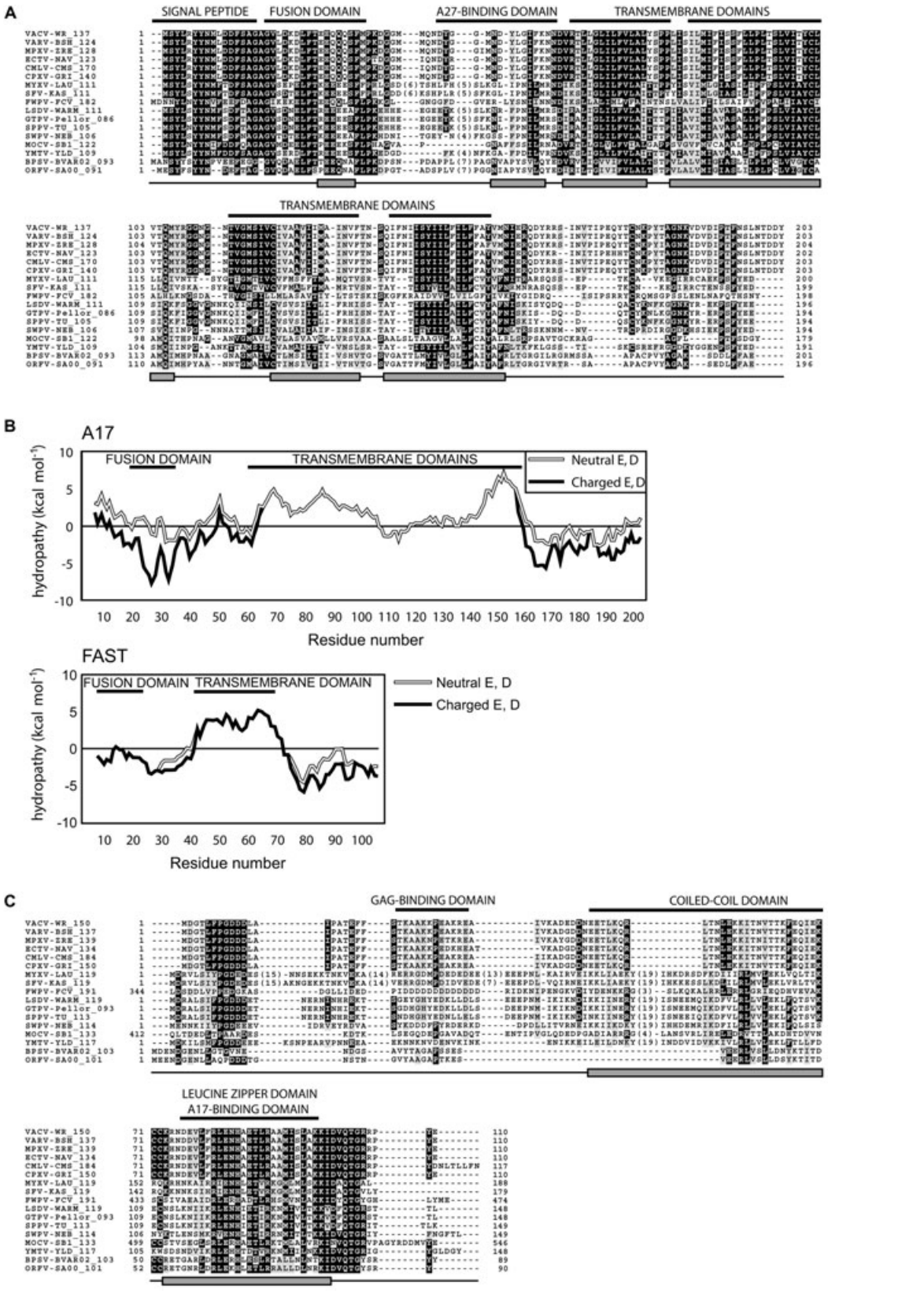
A
SIGNAL PEPTIDE
FUSION DOMAIN
A27-BINDING DOMAIN
TRANSMEMBRANE DOMAINS
VACV-WR_137
VARV-BSH_124
MPXV-ZRE_128
ECTV-NAV_123
CMLV-CMS_170
CPXV-GRI_140
MYXV-LAU_111
SFV-KAS_111
FWPV-FCV_182
LSDV-WARM_111
GTPV-Pellor_086
SPPV-TU_105
SWPV-NEB_106
MOCV-SB1_122
YMTV-YLD_109
BPSV-BVAR02_093
ORFV-SA00_091
TRANSMEMBRANE DOMAINS
B
A17
FUSION DOMAIN
TRANSMEMBRANE DOMAINS
Neutral E, D
Charged E, D
hydropathy (kcal mol-1)
Residue number
FAST
FUSION DOMAIN
TRANSMEMBRANE DOMAIN
Neutral E, D
Charged E, D
hydropathy (kcal mol-1)
Residue number
C
GAG-BINDING DOMAIN
COILED-COIL DOMAIN
LEUCINE ZIPPER DOMAIN
A17-BINDING DOMAIN

Fig. 8. Bioinformatic analysis of A17 and A27 proteins.
A. Sequence analysis and secondary structure predictions of A17. Sequences of homologous proteins from representative species were extracted from the Poxvirus Bioinformatics Resource Center (Lefkowitz *et al*., 2005) and aligned with MUSCLE (Edgar, 2004): VACV-WR, vaccinia virus strain WR; VARV-BSH, variola major virus strain Bangladesh-1975; MPXV-ZRE, monkeypox virus strain Zaire-96-I-16; ECTV-NAV, ectromelia virus strain Naval; CMLV-CMS, camelpox virus CMS; CPXV-GRI, cowpox virus strain GRI-90; MYXV-LAU, myxoma virus strain Lausanne; SFV-KAS, rabbit fibroma virus; FWPV-FCV, fowlpox virus strain fowlpox challenge virus; LSDV-WARM, lumpy skin disease virus isolate Neethling Warmbaths; GTPV-Pellor, goatpox virus strain Pellor; SPPV-TU, sheeppox virus strain TU-V02127; SWPV-NEB, swinepox virus isolate 17077-99; MOCV-SB1, molluscum contagiosum virus subtype 1; YMTV-YLD, yaba-like disease virus; BPSV-BVAR02, bovine papular stomatitis virus strain BV-AR02; ORFV-SA00, orf virus strain OV-SA00. Shading indicates degree of sequence similarity. The extents of A17 domains described in the text are indicated above the alignments. Transmembrane domains were predicted with TMHMM (Krogh *et al*., 2001). At the bottom of the alignments secondary structure predictions with PsiPred (Jones, 1999) are shown: grey boxes represent α-helices.
B. Wimley–White interfacial hydrophobicity (WWIH) score for A17 and FAST proteins. The WWIH measures the ability of a peptide to partition into the interfacial region of the lipid bilayer. A window length of 11 has been used. Scores considering glutamic and aspartic residues as charged at pH 7 and neutral at acid pH are shown.
C. Sequence analysis and secondary structure predictions of A27. Sequences of homologous proteins from representative species were extracted from the Poxvirus Bioinformatics Resource Center (Lefkowitz *et al*., 2005) and aligned with MUSCLE (Edgar, 2004). Abbreviations are like in (A). Shading indicates degree of sequence similarity. The extents of A27 domains described in the text are indicated above the alignments. At the bottom of the alignments secondary structure predictions with PsiPred (Jones, 1999) are shown: grey boxes represent α-helices.

best-studied models. However, in large DNA viruses like herpesvirus, more than a single viral envelope protein is involved in fusion (Colman and Lawrence, 2003; Sollner, 2004; Kielian and Rey, 2006). In poxviruses, an entry/fusion complex of at least eight proteins has been identified by genetic analysis (Moss, 2006). A second complex formed by A27 together with two other membrane proteins, A17 and A14, was also described by our group in VACV based on the ability of mAbs to block A27-mediated virus-to-cell fusion and to immunoprecipitate a complex (Rodriguez *et al*., 1987; Vazquez and Esteban, 1999). Because A17 is a partner of A27 on the membrane surface, we tested their putative fusion activity by their coexpression in heterologous systems. In this way, fusion activity could be characterized in the absence of other VACV proteins. Some of these systems have been successfully used with a number of different viral and cellular fusion proteins (Forzan *et al*., 2004; Dawe *et al*., 2005).

A pH-dependent cell-to-cell fusion process was observed in 293T human cells coexpressing A17 and A27. Fusion was demonstrated by microscopic studies and by a functional quantitative assay based on cytoplasmic transfer of fluorescent proteins. Furthermore, A27 was intracellularly retained in human cells, and it was found on the cell surface only when coexpressed with A17. This suggested that both proteins formed an intracellular complex that was transported to the cell surface. This complex would be responsible for triggering a pH-induced cell-to-cell fusion, because stable expression of only A17 or A27 failed to induce cell fusion. Surprisingly, only A17 showed fusion activity when overexpressed in insect cells. We currently cannot explain this discrepancy between the two expression systems. One plausible explanation would be that A17 overexpression results in a high A17 surface density, possibly inducing fusion without the need for A27. This is the case of other viral fusion proteins which show cooperativity in fusion activity (Danieli *et al*., 1996). Most interestingly, this allowed us to narrow down the region important for fusion (residues 18–34) with A17 deletion mutants in the ectodomain. Deletion of these residues decreased fusion activity to background levels in insect cells. In fact, fusion assays were performed in the presence of mAbs blocking baculovirus gp64 as previously described (Lu *et al*., 2002). Consequently, cells infected with wild-type recombinant baculovirus or expressing A27 did not show fusion. Most interestingly, the ability of the A17 fusion domain to insert into membranes was predicted to increase in acid pH, providing a potential mechanistic explanation for pH-dependent cell fusion.

All the experimental evidence suggested that A17 and A27 were part of a membrane-associated protein complex with fusion activity. Therefore, the A17–A27 complex could in principle be compared with known well-characterized fusion proteins. So far, two main structural classes of viral fusion proteins have been described (Eckert and Kim, 2001; Sollner, 2004; Kielian and Rey, 2006). Class I fusion proteins are homotrimers of two subunits originated from the cleavage of a common precursor, exemplified by influenza virus HA1 and HA2 and HIV-1 gp41 and gp120 proteins. In these proteins, the first globular subunit binds to the viral host receptor and lies on top of the second subunit. The second subunit is a type I membrane protein, composed of α-helices with a coiled-coil motif responsible for the formation of trimers. This subunit contains a fusogenic peptide usually at its N-terminus. The fusogenic peptide is hidden in the core of the trimer, and receptor binding or low pH triggers the exposure of the peptide, which inserts in the host membrane causing fusion between host and viral membranes. Class II fusion proteins, exemplified by flavivirus E and alphavirus E1 proteins, are formed by three domains mostly composed of beta-sheets. They are found as dimers with the fusion peptide hidden in the dimer interface. Upon low pH or receptor binding, the fusion

protein is reorganized as a homotrimer. Then, membrane fusion takes place by a class I-like mechanism. In addition to class I and class II fusion proteins, other types have been described, such as the integral membrane FAST proteins. These proteins present a myristoylated N-terminal ectodomain with a slightly hydrophobic patch, a transmembrane domain and a C-terminal domain containing a basic stretch followed by a polyproline stretch (Shmulevitz and Duncan, 2000).

Attending to the experimental data presented in this work, associated A17–A27 proteins are likely to be a fusion complex. Considering this, the A17–A27 complex would contain essentially the same elements as type I fusion proteins. The membrane-anchoring domain and the fusion peptide reside in A17, while the oligomerization domain and the target membrane-attachment domain are in A27. Nevertheless, A17 alone induced fusion after overexpression in insect cells. In fact, in this regard together with the relatively low hydrophobicity of the fusion peptide, A17 could be compared to FAST-like proteins (Fig. 8). In any case, A17 fusion domain does not resemble any of the well-characterized fusion peptides, suggesting that A17 could be considered a new type of fusion protein.

Concluding, we propose the following working model for A17–A27-mediated cell-to-cell fusion based on the experimental evidence provided in this work. First, A17 and A27 would be transported to the cell membrane as a complex in which A27 remains attached to A17, as shown in mammalian cell lines stably coexpressing both proteins and in previous biochemical binding assays. We hypothesize that binding of A27 to glycosaminoglycans on neighbouring cells would place cells in close proximity. This would explain the fusion inhibition using A27-specific antibodies published by our group. Then, A17 would induce cell-to-cell fusion after a pH drop, because only A17 was shown to possess fusion activity when overexpressed in insect cells. The region important for fusion is present between residues 18 and 34 of A17 ectodomain, because their removal abrogates A17 fusion activity. Finally, as suggested by bioinformatic techniques, a pH drop would increase the capacity of the identified fusion domain to insert in the cell membrane by increasing its hydrophobicity. The validity of this working model is currently under investigation in heterologous systems and in the context of vaccinia infection.

The membrane of MV contains another entry/fusion complex and the virus can gain access to the cytoplasm of the cells by direct fusion and endosomal pathways. A cellular receptor has not been identified yet, probably reflecting the different strategies for virus penetration and delivery of cores into the cell cytoplasm. To our knowledge, this is the first time in which direct fusion activity has been shown for two VACV proteins in the absence of other VACV proteins.

Experimental procedures

Cells and viruses

African green monkey kidney cells (BSC40) and human embryonic kidney 293T cells were grown in Dulbecco's modified Eagle's medium (DMEM) supplemented with 10% fetal calf serum (FCS), at 37°C in a 5% CO_2 atmosphere. Insect Sf21 cells (Invitrogen) were grown at 28°C in T100 Medium supplemented with 10% FCS. 293T cells stably expressing GFP (293T-GFP) or the RFP variant cherry fluorescent protein (293T-RFP) were obtained by transduction with lentivectors encoding GFP or RFP, and selected by three rounds of cloning by limiting dilution (D. Escors *et al*. unpublished).

Vaccinia virus Western Reserve (WR) strain (ATCC VR-1354) DNA was purified as described (Cabrera and Esteban, 1978), and it was used as a template for amplification and cloning of A17 and A27 genes.

Recombinant baculoviruses were obtained using the Bac-to-bac expression system (Invitrogen). All steps in construction, amplification and titration of baculovirus stocks were performed according to the manufacturer's instructions.

Vesicular stomatits virus G glycoprotein-pseudotyped lentivectors were produced by co-transfecting each pHV-SIN-CSGW lentivector plasmid encoding A17 or A27 with packaging plasmids p8.91 and pMDG in 293T cells, and lentivectors were concentrated 100-fold by ultracentrifugation and titrated by quantitative polymerase chain reaction (PCR) as described (Rowe *et al*., 2006; Selden *et al*., 2007).

Plasmids

A17 gene was amplified by PCR from VV DNA, using synthetic primers introducing BamHI (A17 forward primer 5′-GCGGGA TCCATGAGTTATTTAAGATAT-3′) and HindIII (A17 reverse primer 5′-GCGAAGCTTTTAATAATCGTCCTGTTAAATG-3′). A27 gene was similarly amplified by PCR as described above using a forward primer (5′-GCGGGATCCATGGACGGAACTCTTTTCC-3′) and a reverse primer (5′-GCGAAGCTTTTACTCATATGGG CGCCGTCC-3′). Genes were digested with BamHI and HindIII and cloned into the vector pBluescript (Fermentas). The two genes were subcloned into pCIneo (Promega) under the control of the cytomegalovirus early intermediate promoter, generating plasmids pCIneo-A27 and pCIneo-A17. A17 and A27 were also subcloned into pFastBac Dual under the control of p10 and polyhedrin promoters. In this case, the baculovirus gp64 signal peptide sequence was introduced in A17 using the forward primer 5′-GCGAGATCTAAAACATGGTAAGCGCTATTGTTTTAT ATGTGCTTTTGGCGGCGGCGGCGC-3′, and reverse primer 5′-TCTGGATCCGCGGCCGCAAAGGCAGAATGCGCCGCCGC CGCCAAAAGCACATATAAAACA-3′. A17 deletion mutants were generated by overlap extension PCR (Pogulis *et al*., 1996) using synthetic primers and pFastBac-A17 as a template. Briefly, PCR products were obtained with the A17 forward primer together with each corresponding reverse-sense primer containing the deletion, or with the A17 reverse-sense primer with each corresponding forward primer containing the deletion. The following mutants were obtained: A17Δ18-25 was generated by deleting the sequence coding for amino acids 18–25, both included in the deletion, using forward (5′-GCTCTCTCAGCGGCCGCGACAGA GGAACAGCAGCCATCG-3′) and reverse (5′-GCGAGCTTTTAA

TAATCGTCCTGTTAAATG-3′) primers. A17Δ21-34 was generated with forward and reverse primers 5′-GGTGCTGGAGTGCT TCCTAAAGATGGAGGTATGATG-3′ and 5′-ACCTCCATCTTTA GGAAGCACTCCAGCACCCGCAGA-3′. A17Δ31-45 was generated with forward and reverse primers 5′-ACAGAGGAACAGC AGGGAGGAATGAATGATTATTTG-3′ and 5′-ATCATTCATTCCT CCCTGCTGTTCCTCTGTAAATAA-3′. During cloning of the previous mutant, two independent mutations were found in some clones, resulting in the amino-acid changes D32 to N, or Y46 to N. These mutants A17Δ31-45 D23→N and A17Δ31-45 were also used. A17Δ44-59 mutant was generated using a forward primer 5′-GGTATGATGCAAAACGTTAGAACGTTACTCGGTTT G-3′ and a reverse primer 5′-GAGTAACGTTCTAACGTTTTGCA TCATACCTCCATC-3′. Mutant genes were cloned into pFastBac Dual restricted with BamHI and HindIII. All constructs were verified by sequencing.

A17 and A27 genes were cloned in the self-inactivating lentivector backbone pHV-SIN-CSGW (Rowe *et al*., 2006; Selden *et al*., 2007) under the control of the SFFV promoter from pCIneo-A17 and pCIneo-A27 plasmids digested with BamHI and NotI.

Antibodies

A27-specific C3 monoclonal antibody (mAb) and A17-specific rabbit polyclonal serum have been previously described (Rodriguez *et al*., 1985; 1995). Baculovirus gp64-specific monoclonal antibodies were kindly provided by Dr I. Jones (Lu *et al*., 2002). Goat anti-rabbit and goat anti-mouse antibodies conjugated to horseradish peroxidase were purchased form Sigma. Rhodamine and FITC-conjugated anti-mouse and anti-rabbit antibodies were purchased from Molecular Probes. TOPRO was purchased from Molecular Probes. FITC mouse IgG1 kappa and PE-hamster IgG isotype standards were purchased from Pharmingen.

A17 and A27 expression in heterologous systems

Transient transfection with pCIneo plasmids was performed in 293T cells using Lipofectamine 2000 following the manufacturer's instructions (Invitrogen). Briefly, cells were grown in 60-mm-diameter culture plates and were transfected with 4 μg of the indicated plasmids. At 24 h post transfection, cells were seeded in 24-well plates on coverslips at a density of 2×10^5 per well, and cultivated for another 48 h. Transfected cells were processed at 72 h post transfection for confocal immunofluorescence microscopy analysis, or after fusion induction.

To express A17 and A27 genes in insect cells, Sf21 cells were infected with recombinant baculoviruses at a multiplicity of infection (moi) of 5. Between 36 and 48 h post infection, the cells were processed for fusion assays and confocal immunofluorescence microscopy.

For A17- and A27-stable expression in 293T cells, cells were transduced with the indicated lentivectors at a moi of 20 in M24 well plates (NUNC), as described (Rowe *et al*., 2006; Selden *et al*., 2007). Cells were grown at 37°C and kept in culture for a maximum of 1 month.

Cell fusion assay

Transfected 293T cells or cells stably expressing A17 and A27 were incubated at 37°C in DMEM complemented with 10% FCS for 72 h prior to cell fusion induction. Then, cells were washed with PBS or 20 mM sodium acetate, 150 mM NaCl (pH 5.5) and incubated in these buffers for 3 min. Then, cells were washed with DMEM containing 2% FCS, and left in fresh medium. Cells were incubated for 6 h and processed for confocal immunomicroscopy or cytoplasmic transfer assays as described below. Fusion was induced in insect cells with the following modifications. Briefly, Sf21 cells were seeded on coverslips and infected with the recombinant baculoviruses at a moi of 5. Cells were washed 48 h post infection with TC 100 medium without serum, and gp64-specific mAbs were added at a final 1:5000 dilution. After 1 h incubation, the medium was removed and fusion was induced as described above. Then, cells were further incubated in TC medium containing 2% FCS for 6 h and examined by phase-contrast microscopy and confocal immunofluorescence microscopy.

Confocal immunofluorescence microscopy

Briefly, cells were fixed with 4% paraformaldehyde, permeabilized with 0.02% saponin in PBS, for 15 min at RT. After blocking with 20% FCS in PBS, cells were incubated with A27 and A17-specific antibodies for 1 h in blocking buffer. Cells were washed twice and rhodamine-conjugated rabbit anti-mouse or FITC-conjugated goat anti-rabbit antibodies were added at the appropriate dilutions for 1 h, in the presence of ToPro to stain nuclei. Cells were washed twice and coverslips were mounted in ProLong (Molecular Probes). Representative pictures of cell sections and whole projections were obtained using Bio-Rad Radiance 2100 confocal laser microscope.

Living 293T-GFP and 293T-RFP cells transduced with lentivectors encoding A17 or A27 were also observed by fluorescence confocal microscopy using specific filters to detect GFP and RFP.

Surface staining, intracellular staining and flow cytometry

Sf21 cells were infected with recombinant baculoviruses encoding A17 wild-type and mutant genes, as described above. At 48 h post infection, cell cultures were collected, washed with PBS and fixed with 4% paraformaldehyde solution. Non-permeabilized cells were washed and incubated in blocking solution. Then, cells were incubated with A17-specific antibodies for 30 min. Cells were washed and incubated with FITC-conjugated anti-rabbit antibodies. Labelled cells were then analysed in a FACSscan (Becton Dickinson, Mountain View, CA). Uninfected cells were stained as negative controls to set up gates in dot plots and histograms.

Non-permeabilized lentivector-transduced 293T cells were surfaced labelled with specific antibodies as described before (Rowe *et al*., 2006; Selden *et al*., 2007). Briefly, after staining with A17- and A27-specific antibodies, cells were incubated with FITC-conjugated rabbit anti-mouse antibodies or PE-conjugated rat anti-rabbit antibodies (Pharmingen). Unfixed, viable stained 293T cells were gated in a forward/scatter dot plot, and FITC or PE-fluorescence intensity was plotted. To set up gates in dot plots and histograms, FITC and PE isotype standards were used. Untransduced stained 293T cells were used as negative controls to set up voltage conditions and gates. Stained cells were analysed in a BD LSR flow cytometer using appropriate channels for

FITC and PE detection. For GFP and RFP detection, gates were established from 293T cells, and voltage conditions and compensations were established.

Intracellular staining for A17 and A27 in lentivector-transduced 293T cells was performed using the Cytofix/cytoperm kit following the manufacturer's recommendations.

Cytoplasmic transfer of fluorescent proteins

A functional quantitative fusion assay was set up based on cytoplasmic transfer between RFP-containing cells and GFP-containing cells. Briefly, 293T-GFP or 293T-RFP cells were transduced with lentivectors encoding A17 and A27. These lines were maintained separately in cell cultures. Then, cells were mixed 1:1 and allowed to attach to a culture plate surface for at least 2 h. After attachment, pH-induced fusion was performed as described above, and cells were incubated from 2 to 4 h to allow fusion. Cell fusions were detected as GFP^+ RFP^+ events in living cells either by confocal fluorescent microscopy with specific filters for GFP or RFP detection, or by flow cytometry as described above.

Statistical analyses

The percentage of syncytia was calculated as the number of nuclei involved in fusion events compared with the total number of nuclei recorded in randomly chosen microscopy fields. In 293T cells transiently transfected, a total number of 700 nuclei was counted due to low transfection efficiencies. In the baculovirus system, a total number of 3000 nuclei were recorded. The percentage of syncytia was normally distributed as determined by the chi-squared test. Therefore, the fusiogenic activity of each mutant was compared using the parametric ANOVA test for multiple comparisons, and using Tukey's test in selected cases further two-paired comparisons.

Acknowledgements

We thank Dr Silvia Gutierrez for help in confocal microscopy and flow cytometry analysis, Victoria Jiménez for excellent technical assistance and Dr Ian Jones of University of Reading (UK) for monoclonal antibodies recognizing gp64–baculovirus fusion protein. We are indebted to Professor Mary Collins, Director MRC/UCL Centre for Medical Molecular Virology, London, for her support with the experiments on lentivirus vectors and fluorescence cells. This investigation was supported by the Spanish Ministry of Education and Science (BIO2002-03246), the EU (QLK2-2002-01687) and Fundación Botín. G.K. was supported by a fellowship from Comunidad de Madrid, and D.E. was funded by a Postdoctoral Marie Curie Fellowship.

References

Armstrong, J.A., Metz, D.H., and Young, M.R. (1973) The mode of entry of vaccinia virus into L cells. *J Gen Virol* **21:** 533–537.

Betakova, T., and Moss, B. (2000) Disulfide bonds and membrane topology of the vaccinia virus A17L envelope protein. *J Virol* **74:** 2438–2442.

Betakova, T., Wolffe, E.J., and Moss, B. (1999) Membrane topology of the vaccinia virus A17L envelope protein. *Virology* **261:** 347–356.

Cabrera, C.V., and Esteban, M. (1978) Procedure for purification of intact DNA from vaccinia virus. *J Virol* **25:** 442–445.

Carter, G.C., Law, M., Hollinshead, M., and Smith, G.L. (2005) Entry of the vaccinia virus intracellular mature virion and its interactions with glycosaminoglycans. *J Gen Virol* **86:** 1279–1290.

Chang, A., and Metz, D.H. (1976) Further investigations on the mode of entry of vaccinia virus into cells. *J Gen Virol* **32:** 275–282.

Chung, C.S., Hsiao, J.C., Chang, Y.S., and Chang, W. (1998) A27L protein mediates vaccinia virus interaction with cell surface heparan sulfate. *J Virol* **72:** 1577–1585.

Collins, M.K., and Cerundolo, V. (2004) Gene therapy meets vaccine development. *Trends Biotechnol* **22:** 623–626.

Colman, P.M., and Lawrence, M.C. (2003) The structural biology of type I viral membrane fusion. *Nat Rev Mol Cell Biol* **4:** 309–319.

Corcoran, J.A., Syvitski, R., Top, D., Epand, R.M., Epand, R.F., Jakeman, D., and Duncan, R. (2004) Myristoylation, a protruding loop, and structural plasticity are essential features of a nonenveloped virus fusion peptide motif. *J Biol Chem* **279:** 51386–51394.

Danieli, T., Pelletier, S.L., Henis, Y.I., and White, J.M. (1996) Membrane fusion mediated by the influenza virus hemagglutinin requires the concerted action of at least three hemagglutinin trimers. *J Cell Biol* **133:** 559–569.

Dawe, S., Corcoran, J.A., Clancy, E.K., Salsman, J., and Duncan, R. (2005) Unusual topological arrangement of structural motifs in the baboon reovirus fusion-associated small transmembrane protein. *J Virol* **79:** 6216–6226.

Doms, R.W., Blumenthal, R., and Moss, B. (1990) Fusion of intra- and extracellular forms of vaccinia virus with the cell membrane. *J Virol* **64:** 4884–4892.

Eckert, D.M., and Kim, P.S. (2001) Mechanisms of viral membrane fusion and its inhibition. *Annu Rev Biochem* **70:** 777–810.

Edgar, R.C. (2004) MUSCLE: multiple sequence alignment with high accuracy and high throughput. *Nucleic Acids Res* **32:** 1792–1797.

Ericsson, M., Cudmore, S., Shuman, S., Condit, R.C., Griffiths, G., and Locker, J.K. (1995) Characterization of ts 16, a temperature-sensitive mutant of vaccinia virus. *J Virol* **69:** 7072–7086.

Forzan, M., Wirblich, C., and Roy, P. (2004) A capsid protein of nonenveloped Bluetongue virus exhibits membrane fusion activity. *Proc Natl Acad Sci USA* **101:** 2100–2105.

Gething, M.J., McCammon, K., and Sambrook, J. (1986) Expression of wild-type and mutant forms of influenza hemagglutinin: the role of folding in intracellular transport. *Cell* **46:** 939–950.

Gong, S.C., Lai, C.F., and Esteban, M. (1990) Vaccinia virus induces cell fusion at acid pH and this activity is mediated by the N-terminus of the 14-kDa virus envelope protein. *Virology* **178:** 81–91.

Hsiao, J.C., Chung, C.S., and Chang, W. (1999) Vaccinia

virus envelope D8L protein binds to cell surface chondroitin sulfate and mediates the adsorption of intracellular mature virions to cells. *J Virol* **73:** 8750–8761.

Janeczko, R.A., Rodriguez, J.F., and Esteban, M. (1987) Studies on the mechanism of entry of vaccinia virus in animal cells. *Arch Virol* **92:** 135–150.

Jaysinghe, S., Hristova, K., Wimley, W., Snider, C., and White, S.H. (2006) Membrane Protein Explorer (MPEx). Available at: http://blanco.biomol.uci.edu/mpex.

Jones, D.T. (1999) Protein secondary structure prediction based on position-specific scoring matrices. *J Mol Biol* **292:** 195–202.

Kielian, M., and Rey, F.A. (2006) Virus membrane-fusion proteins: more than one way to make a hairpin. *Nat Rev Microbiol* **4:** 67–76.

Kim, D.E., Chivian, D., and Baker, D. (2004) Protein structure prediction and analysis using the Robetta server. *Nucleic Acids Res* **32:** W526–W531.

Kochan, G., Tyborowska, J., and Szewczyk, B. (1993) Expression of animal virus genes using baculovirus AcNPV. *Acta Biochim Pol* **40:** 1–3.

Kochan, G., Gonzalez, D., and Rodriguez, J.F. (2003) Characterization of the RNA-binding activity of VP3, a major structural protein of infectious bursal disease virus. *Arch Virol* **148:** 723–744.

Krijnse-Locker, J., Schleich, S., Rodriguez, D., Goud, B., Snijder, E.J., and Griffiths, G. (1996) The role of a 21-kDa viral membrane protein in the assembly of vaccinia virus from the intermediate compartment. *J Biol Chem* **271:** 14950–14958.

Krogh, A., Larsson, B., von Heijne, G., and Sonnhammer, E.L. (2001) Predicting transmembrane protein topology with a hidden Markov model: application to complete genomes. *J Mol Biol* **305:** 567–580.

Kurowski, M.A., and Bujnicki, J.M. (2003) GeneSilico protein structure prediction meta-server. *Nucleic Acids Res* **31:** 3305–3307.

Kyte, J., and Doolittle, R.F. (1982) A simple method for displaying the hydropathic character of a protein. *J Mol Biol* **157:** 105–132.

Lai, C.F., Gong, S.C., and Esteban, M. (1990) Structural and functional properties of the 14-kDa envelope protein of vaccinia virus synthesized in *Escherichia coli*. *J Biol Chem* **265:** 22174–22180.

Law, M., Carter, G.C., Roberts, K.L., Hollinshead, M., and Smith, G.L. (2006) Ligand-induced and nonfusogenic dissolution of a viral membrane. *Proc Natl Acad Sci USA* **103:** 5989–5994.

Lefkowitz, E.J., Upton, C., Changayil, S.S., Buck, C., Traktman, P., and Buller, R.M. (2005) Poxvirus Bioinformatics Resource Center: a comprehensive Poxviridae informational and analytical resource. *Nucleic Acids Res* **33:** D311–D316.

Lin, C.L., Chung, C.S., Heine, H.G., and Chang, W. (2000) Vaccinia virus envelope H3L protein binds to cell surface heparan sulfate and is important for intracellular mature virion morphogenesis and virus infection in vitro and in vivo. *J Virol* **74:** 3353–3365.

Lin, T.H., Chia, C.M., Hsiao, J.C., Chang, W., Ku, C.C., Hung, S.C., and Tzou, D.L. (2002) Structural analysis of the extracellular domain of vaccinia virus envelope protein, A27L, by NMR and CD spectroscopy. *J Biol Chem* **277:** 20949–20959.

Lu, W., Chapple, S.D., Lissini, O., and Jones, I.M. (2002) Characterization of a truncated soluble form of the baculovirus (AcMNPV) major envelope protein Gp64. *Protein Expr Purif* **24:** 196–201.

Maa, J.S., Rodriguez, J.F., and Esteban, M. (1990) Structural and functional characterization of a cell surface binding protein of vaccinia virus. *J Biol Chem* **265:** 1569–1577.

Mercer, J., and Traktman, P. (2003) Investigation of structural and functional motifs within the vaccinia virus A14 phosphoprotein, an essential component of the virion membrane. *J Virol* **77:** 8857–8871.

Moss, B. (2001) *Poxviridae. The Viruses and Their Replication*. Philadelphia, PA: Lippincott Williams & Wilkins.

Moss, B. (2006) Poxvirus entry and membrane fusion. *Virology* **344:** 48–54.

Nieva, J.L., and Suarez, T. (2000) Hydrophobic–at interface regions in viral fusion protein ectodomains. *Biosci Rep* **20:** 519–533.

Ojeda, S., Senkevich, T.G., and Moss, B. (2006) Entry of vaccinia virus and cell-cell fusion require a highly conserved cysteine-rich membrane protein encoded by the A16L gene. *J Virol* **80:** 51–61.

Pogulis, R.J., Vallejo, A.N., and Pease, L.R. (1996) *In vitro* recombination and mutagenesis by overlap extension PCR. In *In Vitro Mutagenesis Protocols*. Trower, M.K. (ed.). Totwa: Humana Press, pp. 167–176.

Rodriguez, D., Rodriguez, J.R., and Esteban, M. (1993) The vaccinia virus 14-kilodalton fusion protein forms a stable complex with the processed protein encoded by the vaccinia virus A17L gene. *J Virol* **67:** 3435–3440.

Rodriguez, D., Esteban, M., and Rodriguez, J.R. (1995) Vaccinia virus A17L gene product is essential for an early step in virion morphogenesis. *J Virol* **69:** 4640–4648.

Rodriguez, D., Risco, C., Rodriguez, J.R., Carrascosa, J.L., and Esteban, M. (1996) Inducible expression of the vaccinia virus A17L gene provides a synchronized system to monitor sorting of viral proteins during morphogenesis. *J Virol* **70:** 7641–7653.

Rodriguez, J.F., and Esteban, M. (1987) Mapping and nucleotide sequence of the vaccinia virus gene that encodes a 14-kilodalton fusion protein. *J Virol* **61:** 3550–3554.

Rodriguez, J.F., and Smith, G.L. (1990) IPTG-dependent vaccinia virus: identification of a virus protein enabling virion envelopment by Golgi membrane and egress. *Nucleic Acids Res* **18:** 5347–5351.

Rodriguez, J.F., Janeczko, R., and Esteban, M. (1985) Isolation and characterization of neutralizing monoclonal antibodies to vaccinia virus. *J Virol* **56:** 482–488.

Rodriguez, J.F., Paez, E., and Esteban, M. (1987) A 14,000-Mr envelope protein of vaccinia virus is involved in cell fusion and forms covalently linked trimers. *J Virol* **61:** 395–404.

Rodriguez, J.R., Risco, C., Carrascosa, J.L., Esteban, M., and Rodriguez, D. (1997) Characterization of early stages in vaccinia virus membrane biogenesis: implications of the 21-kilodalton protein and a newly identified 15-kilodalton envelope protein. *J Virol* **71:** 1821–1833.

Rodriguez, J.R., Risco, C., Carrascosa, J.L., Esteban, M.,

and Rodriguez, D. (1998) Vaccinia virus 15-kilodalton (A14L) protein is essential for assembly and attachment of viral crescents to virosomes. *J Virol* **72:** 1287–1296.
Rowe, H.M., Lopes, L., Ikeda, Y., Bailey, R., Barde, I., Zenke, M., *et al.* (2006) Immunization with a lentiviral vector stimulates both CD4 and CD8 T cell responses to an ovalbumin transgene. *Mol Ther* **13:** 310–319.
Selden, C., Mellor, N., Rees, M., Laurson, J., Kirwan, M., Escors, D., *et al.* (2007) Growth factors improve gene expression after lentiviral transduction in human adult and fetal hepatocytes. *J Gene Med* **9:** 67–76.
Senkevich, T.G., and Moss, B. (2005) Vaccinia virus H2 protein is an essential component of a complex involved in virus entry and cell-cell fusion. *J Virol* **79:** 4744–4754.
Senkevich, T.G., Ward, B.M., and Moss, B. (2004a) Vaccinia virus entry into cells is dependent on a virion surface protein encoded by the A28L gene. *J Virol* **78:** 2357–2366.
Senkevich, T.G., Ward, B.M., and Moss, B. (2004b) Vaccinia virus A28L gene encodes an essential protein component of the virion membrane with intramolecular disulfide bonds formed by the viral cytoplasmic redox pathway. *J Virol* **78:** 2348–2356.
Senkevich, T.G., Ojeda, S., Townsley, A., Nelson, G.E., and Moss, B. (2005) Poxvirus multiprotein entry-fusion complex. *Proc Natl Acad Sci USA* **102:** 18572–18577.
Shmulevitz, M., and Duncan, R. (2000) A new class of fusion-associated small transmembrane (FAST) proteins encoded by the non-enveloped fusogenic reoviruses. *EMBO J* **19:** 902–912.
Smith, G.L., and Vanderplasschen, A. (1998) Extracellular enveloped vaccinia virus. Entry, egress, and evasion. *Adv Exp Med Biol* **440:** 395–414.
Smith, G.L., Vanderplasschen, A., and Law, M. (2002) The formation and function of extracellular enveloped vaccinia virus. *J Gen Virol* **83:** 2915–2931.
Sollner, T.H. (2004) Intracellular and viral membrane fusion: a uniting mechanism. *Curr Opin Cell Biol* **16:** 429–435.
Townsley, A.C., Senkevich, T.G., and Moss, B. (2005a) Vaccinia virus A21 virion membrane protein is required for cell entry and fusion. *J Virol* **79:** 9458–9469.
Townsley, A.C., Senkevich, T.G., and Moss, B. (2005b) The product of the vaccinia virus L5R gene is a fourth membrane protein encoded by all poxviruses that is required for cell entry and cell-cell fusion. *J Virol* **79:** 10988–10998.
Townsley, A.C., Weisberg, A.S., Wagenaar, T.R., and Moss, B. (2006) Vaccinia virus entry into cells via a low-pH-dependent endosomal pathway. *J Virol* **80:** 8899–8908.
Vazquez, M.I., and Esteban, M. (1999) Identification of functional domains in the 14-kilodalton envelope protein (A27L) of vaccinia virus. *J Virol* **73:** 9098–9109.
Vazquez, M.I., Rivas, G., Cregut, D., Serrano, L., and Esteban, M. (1998) The vaccinia virus 14-kilodalton (A27L) fusion protein forms a triple coiled-coil structure and interacts with the 21-kilodalton (A17L) virus membrane protein through a C-terminal alpha-helix. *J Virol* **72:** 10126–10137.
Wallengren, K., Risco, C., Krijnse-Locker, J., Esteban, M., and Rodriguez, D. (2001) The A17L gene product of vaccinia virus is exposed on the surface of IMV. *Virology* **290:** 143–152.
Wimley, W.C., and White, S.H. (1996) Experimentally determined hydrophobicity scale for proteins at membrane interfaces. *Nat Struct Biol* **3:** 842–848.
Wimley, W.C., Gawrisch, K., Creamer, T.P., and White, S.H. (1996) Direct measurement of salt-bridge solvation energies using a peptide model system: implications for protein stability. *Proc Natl Acad Sci USA* **93:** 2985–2990.
Wolffe, E.J., Moore, D.M., Peters, P.J., and Moss, B. (1996) Vaccinia virus A17L open reading frame encodes an essential component of nascent viral membranes that is required to initiate morphogenesis. *J Virol* **70:** 2797–2808.